The following publication W. Lyu, W. Xu, F. Yang, S. Chen, F. Tan and C. Yu, "Non-Invasive Measurement for Cardiac Variations Using a Fiber Optic Sensor," in IEEE Photonics Technology Letters, vol. 33, no. 18, pp. 990-993, 15 Sept. 2021 is available at https://doi.org/10.1109/LPT.2021.3078757.

Non-invasive Measurement for Cardiac Variations Using a Fiber Optic Sensor

Weimin Lyu**, Wei Xu**, Fangang Yang, Shuyang Chen, Fengze Tan, and Changyuan Yu

***Abstract*—Cardiovascular diseases (CVDs) are very common in modern society, such as atherosclerosis, hypertension, etc., which have a great impact on heart function. Therefore, hospitalization monitoring alone is far from enough. Long-term monitoring of the heart is needed in daily life. The technology of non-invasive monitoring of the cardiovascular system can meet the needs of long-term monitoring of the heart condition, helping to promote the improvement of lifestyle and daily care, reducing the overall risk of developing CVDs. The purpose of this study is to investigate the cardiac response after different exercises using a 3×3 demodulation scheme-based ballistocardiography (BCG) monitoring system. A fiber optic sensor (FOS)-based smart cushion is used to replace the traditional inconvenient electrocardiogram (ECG) for heart rate variability (HRV). The correlation between BCG inter-beat interval (IBI) and ECG IBI is 0.9862, and the RMSE is 0.0139. The BCG signal can assess cardiac contractility by analyzing RJ interval with ECG, which is a practical alternative to the pre-ejection period (PEP).**

***Index Terms*—Optical fibers, Fiber optic sensors, Optical fiber interference, Biomedical transducers.**

I. Introduction

In modern society, medical care is receiving more and more attention, and people are willing to invest more in this field. Monitoring the health of the elderly is essential in an aging society. In the past, many examinations could only be performed by medical staff, but many diseases such as atrial fibrillation (AF), hypertension, myocardial infarction and heart failure require long-term monitoring. These requirements mean that medical services previously limited to hospitals need to gradually extend to people's homes to support their daily medical care.

For people with a high risk of heart disease, regular assessment of their cardiovascular parameters and taking measures at an early stage can reduce the risk of disease. For people with a high risk of heart disease, regular assessment of their cardiovascular parameters, and taking measures at an early stage can reduce their risk of disease. For patients with cardiovascular diseases (such as heart failure), implantable devices are often used for treatment [1, 2]. More and more evidence shows that non-invasive monitoring outside the clinical environment can achieve early detection of CVD risks (such as arteriosclerosis) [3, 4]. But cardiovascular health needs to be judged by many aspects. Parameters such as blood pressure (BP), HRV, and cardiac contractility must be measured accurately. Neither medical nor household equipment can satisfy long-term monitoring in a non-clinical environment. Common devices in the consumer field include ECG [5], PPG [6], smartwatches, etc. These devices can provide more accurate HRV information, but cannot reflect mechanical health information of the cardiovascular system. In the research field, researchers have developed impedance cardiography (ICG) that can measure the mechanical health of the cardiovascular system [7]. However, multiple electrodes need to be attached to the patient during measurement, which causes discomfort, and the equipment is bulky and expensive to purchase, which is not suitable for home monitoring.

BCG is a technique used for non-invasive measurement of the recoil force caused by the blood pumped into the aorta during every heartbeat [8]. This phenomenon was first observed in 1877 by Gordon. He found that the pointer will deflect on both sides of the dial at every heartbeat when standing on an ordinary spring weighing machine [9]. About 60 years after the discovery of BCG, Starr et al. conducted significant research on its measurement equipment. However, due to sensor technology and measurement resolution limitations, research related to BCG almost disappeared in the late 19th century. In the recent two decades, further research on BCG raised again, and various principle-based measuring devices have been designed for BCG data collection [10-14].

Compared with other cardiovascular detection technologies, like ECG and ICG, BCG has the advantages of non-invasive and convenient detection. It is proposed to use it for cardiac diagnosis to achieve the same purpose. The research on the physiological significance of ECG signals is very mature, and the physiological importance of BCG signals is still under further study. This paper attempts to prove that FOS-based BCG can be used as a substitute for ECG, and analyzes the

**These authors contributed equally to this work.

This work is supported by the National Natural Science Foundation of China (Grant 61971372); Research Grants Council, University Grants Committee of Hong Kong (Grant 15200718). (Corresponding author: Changyuan Yu.)

W. Lyu and F. Tan are with Shenzhen Research Institute, The Hong Kong Polytechnic University, Shenzhen, China. (e-mail: weimin.lyu@connect.polyu.hk, f.z.tan@connect.polyu.hk).

W. Xu is with State Key Laboratory of Transient Optics and Photonics, Xi'an Institute of Optics and Precision Mechanics, Chinese Academy of Sciences, Xi'an 710119, China, and is also with University of Chinese Academy of Sciences, Beijing 100049, China (e-mail: xuwei@opt.cn).

F. Yang is with Department of Electrical and Computer Engineering, National University of Singapore, Singapore (e-mail: e0679892@u.nus.edu).

C. Yu and S. Chen are with the Department of Electronic and Information Engineering, The Hong Kong Polytechnic University, Kowloon, Hong Kong (e-mail: changyuan.yu@polyu.edu.hk, shu-yang.chen@connect.polyu.hk).

effects of different intensities of exercise on the heart.

II. Materials and Methods

A. Protocol

In this experiment, the HR signal was calculated separately by ECG (AD 8232) and BCG (FOS) collected at the same time. The HR obtained from ECG is called ECG HR, and the HR obtained from BCG is called BCG HR. We will compare the errors of the two to determine whether the BCG HR analysis based on FOS can be used as a substitute for ECG. The subject was asked to sit on the cushion with the FOS underneath for data acquisition, and to attach three ECG electrodes on the chest and abdomen. Fig. 1 (a) shows the system setup. Before acquiring data, the subject was asked to perform four different exercises after resting for 60 seconds: respiration (RES) exercise, dynamic squat exercise (DSE), Valsalva maneuver (VM), and running exercise. We hope to find the difference in the effects of different intensities of exercise on HR and PEP.

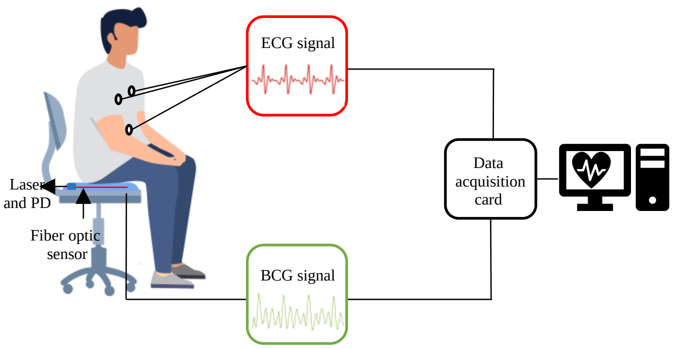

(a)

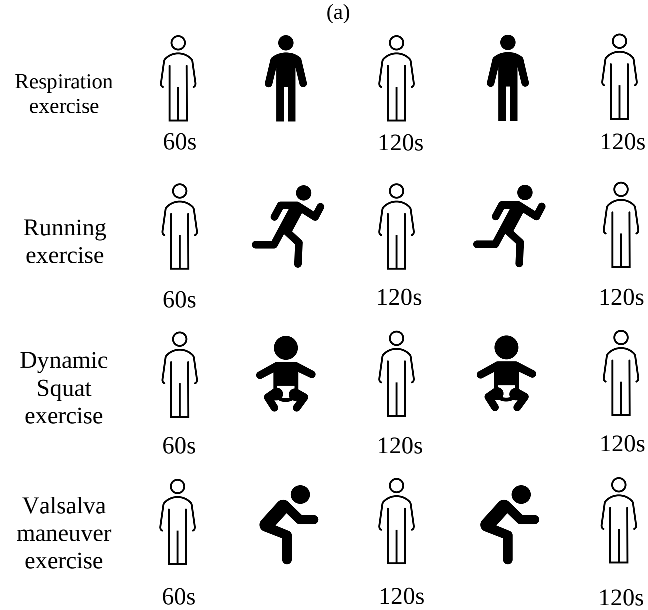

(b)

Fig. 1. (a) System setup, (b) overview protocol.

In Fig. 1 (b), an overview of the experiment is shown. When performing breathing exercises, the subject breathes 6 times per minute (0.1 Hz), and the maximum HRV amplitude can be observed at this breathing rate [15]. The DSE was to perform 40 squats as fast as possible. During VM, the subject expiratory against the mouth closed and the nostrils pinched, which forces air into the eustachian tubes and increases pressure on the inside of the eardrum. This maneuver causes changes in blood pressure and HR and is used in conjunction with other tests to diagnose heart abnormalities and treat various conditions, especially certain abnormal heart rhythms.

B. Sensor structure

In our previous work, the BCG signal measured using a common Mach–Zehnder interferometer (MZI) met signal fading problem [16]. The interferometer should have the highest sensitivity when the optical path difference between the two arms is π/2; and when the phase difference is π, the signal change can hardly be detected. In the experiment, even if the optical path difference between the two arms is adjusted to π/2 in advance, the optical path difference between the two arms cannot be maintained at π/2 in the static state due to the slowly varying random phase drift noise, temperature changes. Considering ease of use and cost, this research proposes a new MZI structure based on a 3 × 3 coupler, as shown in Fig. 2. In this sensor, a 1 × 2 coupler of the traditional MZI is replaced with a 3 × 3 coupler, so that it has three outputs with a phase difference of 120°, and the signals are received by three PDs respectively. The three signals are processed by the circuit and stored in the computer by the data acquisition card.

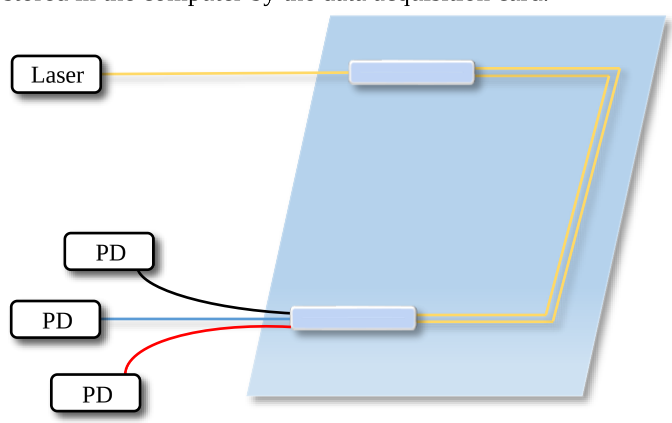

Fig. 2. Optical fiber interferometer based on the 3 × 3 coupler.

The output light intensity of the interferometer is:

$$I_k = D + I_0 \cos[\varphi(t) - (k-1)(2\pi/3)], \quad (1)$$

which, $\varphi(t) = \phi(t) + \psi(t)$, D is the average value of output light intensity, I_0 is the peak intensity of interference fringes, k is the number of the output light path, $k = 1, 2, 3$, $\varphi(t)$ is the phase difference signal of the sensor, that is, the signal to be measured, $\psi(t)$ is the phase difference caused by environmental changes.

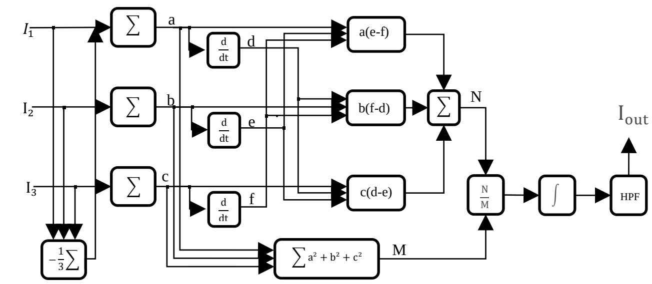

Fig. 3. Demodulation principle.

The demodulation method of the 3×3 coupler scheme is shown in Fig. 3. After differentiation and cross multiplication, the demodulated signal is:

$$N = a(e-f) + b(f-d) + c(d-e) = \frac{3\sqrt{3}}{2} I_0^2 \varphi'(t), \quad (2)$$

In the actual environment, fluctuations in the intensity of the light source and changes in the polarization state will change the value of I_0. In order to eliminate the impact on I_0, first square the three input signals to obtain:

$$M = a^2 + b^2 + c^2 = \frac{3I_0^2}{2}, \quad (3)$$

Then divide (N) by (M) and eliminate I_0^2 to get:

$$P = \frac{N}{M} = \sqrt{3}\varphi'(t), \quad (4)$$

The output after integration operation is:

$$V_{out} = \sqrt{3}\varphi(t) = \sqrt{3}\phi(t) + \psi(t), \quad (5)$$

V_{out} is the output signal of the 3*3 demodulation scheme. Usually, $\psi(t)$ is regarded as a slow change quantity, which can be filtered out through a high-pass filter. Finally, we can get $\phi(t)$, which is the BCG signal used in this paper.

In our new sensor, the light from a 1550 nm distributed feedback laser is injected into the reference fiber and the sensing fiber through a 1×2 coupler. Then, the reference light will interfere with the light in the sensing fiber at the 2×3 coupler. The interference signals are received by three photodetectors (PDs), and the three-channel signals are sampled by a data acquisition card.

C. Data Acquisition

The Analog Input Recorder APP of MATLAB was used to collect the data to the PC through the data acquisition card (USB 6002) of National Instruments. The system acquired all 4 channels (three channels of BCG signals and 1 channel of ECG signals) at a sampling frequency of 5k Hz.

D. Data post-processing

The R peaks of the ECG signal are detected by the "findpeaks" function of MATLAB. The reference IBI is calculated from the RR interval of the ECG. The BCG signals are demodulated using the above scheme and then filtered using a bandpass filter with a lower cut-off frequency of 1.2 Hz and a higher frequency of 35 Hz [17]. This filter can filter out breathing and motion artifacts and get more details about the high frequency part of the BCG (i.e., J peak). The J peak of BCG is detected by the same function. The comparison between the final BCG signal and 3 channels signal is shown in Fig. 4. The top three pictures are three BCG output signals, and the bottom picture is the BCG signal after demodulation. Obviously, all three output signals have signal fading problem in a certain period of time. After demodulation, this problem is solved well.

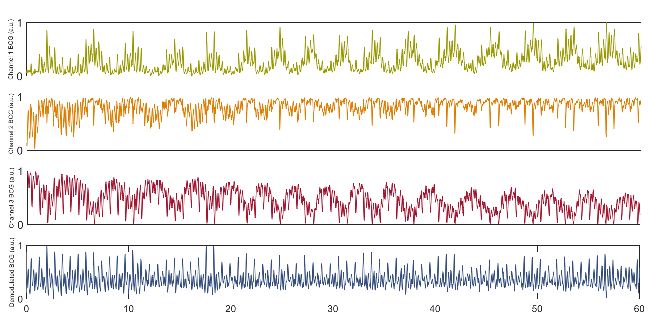

Fig. 4. Comparison between original and demodulation signals.

III. Results and Discussion

The common IBI is calculated from the R-R interval of ECG, called ECG IBI, and used as a reference for IBI validation in this study. The BCG IBI was calculated by the J-J interval. There are a total of 1060 heartbeats in a total of 580s in the four exercises. We use MATLAB to calculate the correlation between the two. The correlation between BCG IBI and ECG IBI is 0.9862, and the RMSE is 0.0139. The IBI used in the analysis of HRV and PEP in this study was calculated by BCG.

Fig. 5 shows the IBI after four different exercises. All exercises increased HR, and the trend was not the same. In Fig. 5 (a), the VM was performed in the 10th second and released strains after 15 seconds, marked with red line. During this period, the HR gradually increases and returned to normal after released strains. The mean value of HR is 0.9381 s. In Fig. 5 (b) and (c), HR gradually slows down from fast. The mean values of DSE and RUN HR are 0.6572 s and 0.5277 s, respectively. Because running is more intense, the measured initial HR is faster. Fig. 5 (d) shows the HR during respiration exercise, and the mean value is 0.8054 s. It increases during inhalation (shortened J–J interval) and decreases during exhalation (extended J–J interval). This is called respiratory sinus arrhythmia (RSA) and reflects changes in cardiac autonomic regulation.

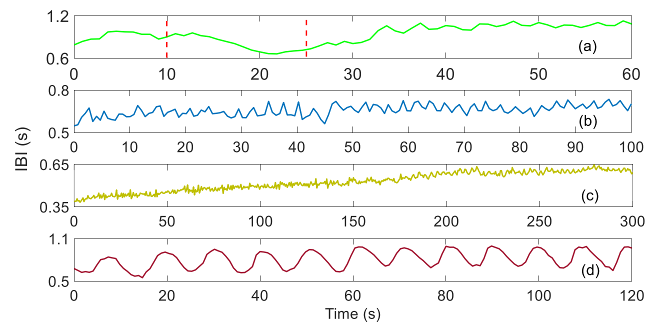

Fig. 5. (a) Valsalva maneuver IBI, (b) dynamic squat exercise IBI, (c) running exercise IBI, (d) respiration exercise IBI.

PEP is one of the systolic time intervals, measured from the Q wave of the ECG to the B wave of the ICG. It represents sympathetic activity and can be used to assess myocardial contractility. Because ICG equipment is expensive and the measurement is complicated, RJ interval is usually used as a substitute for PEP. It is defined as the interval between the R peak of ECG and the J peak of BCG, and has been investigated quantitively that the relationship between the PEP and R-J interval follows [18]:

$$Y_{RJ} = 1.05 \cdot PEP + 138, \quad (6)$$

Fig. 6 shows the PEP after four different exercises. In Fig. 6 (a), when the VM starts, the PEP suddenly became smaller. This phenomenon may be due to deep breathing before the start of VM. During this process, the PEP is almost unchanged, and after released strains, it suddenly decreases and then gradually recovers. Throughout the testing process, the mean value of PEP is 116.344 ms. In Fig. 6 (b), the PEP mean value is 93.9704 ms, it fluctuates violently and shows no obvious trend after DSE. The PEP variation is shown in Fig. 6 (c), the mean value is 63.9383 ms. It fluctuates sharply after running exercise, and the overall trend has gradually increased. In Fig. 6 (d), the PEP mean value is 106.2365 ms, which trend is basically the same as HR during breathing.

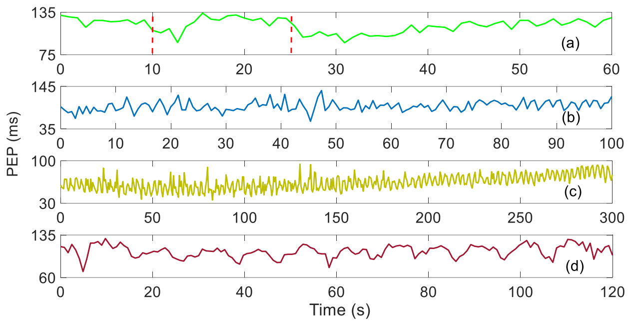

Fig. 6. (a) Valsalva maneuver PEP, (b) dynamic squat exercise PEP, (c) running exercise PEP, (d) respiration exercise PEP.

The goal of this study is to investigate IBI and the PEP variation after different exercises. The extremely high correlation between BCG IBI and ECG IBI shows that the IBI calculated by the J-J interval of BCG is accurate enough for HRV analysis. Because the subject needs to breathe quickly and deeply before VM, the larger mutations in HR and PEP may be caused by breathing in the early stage of VM. After the four exercises, the trends of IBI and PEP seem to show that the two are positively correlated to a certain extent. However, during VM, IBI first decreased and then increased, while PEP remained almost at a normal level. This result shows that PEP is not always consistent with the trend of IBI. Under ideal experimental conditions, the breathing rate during the test period should remain constant. However, experiments have shown that individuals cannot fully breathe following a fixed speed. In addition, swallowing was sometimes observed in a few cases, so there are differences in breathing rate. The change of HR and PEP in each breath is not exactly the same. In the same way, the fluctuations in HR and PEP during the whole test may also be caused by irregular breathing. As we all know, sports exercises will speed up HR. VM is the least intense exercise, so the recovery of HR is the fastest. Due to the short exercise time of DSE, HR does not increase as much as running. However, there are obvious differences in the trend of PEP after the two sport exercises. After DSE, the PEP fluctuates between 59 ms and 135 ms, with a central value of 97 ms. After running exercise, the PEP fluctuates between 30 ms and 100 ms, the central value first decreases from 59 ms to 49 ms, and gradually increases to 78 ms in the next 300 s, and there is a tendency to continue to increase. Both PEP values fluctuate greatly, but there is not much change from the normal value of 110 ms in DSE data (the PEP decreases to about 59 ms after running). It is not sure whether it is related to the exercise kinds, or to the intensity and duration of the exercise. During the RES exercise, IBI fluctuates around 0.8 s (0.6 s-1.0 s), and PEP fluctuates around 97 ms (78 ms-126 ms). Both of them change around the value in the normal resting state. All the changes of IBI and PEP show the variations in a healthy heart pumping under parasympathetic regulation after different exercises.

IV. Conclusion

We have reported a monitoring system for HR and myocardial contractility based on an interferometric FOS. The signal fading has been solved, and long-term monitoring can be carried out. The BCG HRV calculated from the demodulated signal can be used as a new accurate heart condition analysis signal. The analysis of PEP combined with ECG can be a good assessment of myocardial contractility. Thanks to its non-contact measurement, BCG based on FOS will become an important part of heart condition analysis.

References

[1] W. T. Abraham, P. B. Adamson, R. C. Bourge, M. F. Aaron, M. R. Costanzo, L. W. Stevenson, ... & S. Weiner, “Wireless pulmonary artery haemodynamic monitoring in chronic heart failure: a randomised controlled trial”, The Lancet, vol. 377, no. 9766, pp. 658-666, 2011.

[2] A. L. Bui, and G. C. Fonarow, "Home monitoring for heart failure management," Journal of the American College of Cardiology, vol. 59, no. 2, pp. 97-104, 2012.

[3] Determinants of pulse wave velocity in healthy people and in the presence of cardiovascular risk factors: “establishing normal and reference values”.

[4] T. Willum-Hansen, J. A. Staessen, C. Torp-Pedersen, S. Rasmussen, L. Thijs, H. Ibsen, and J. Jeppesen, “Prognostic value of aortic pulse wave velocity as index of arterial stiffness in the general population,” Circulation, vol. 113, no. 5, pp. 664-70, 2006.

[5] D. Dubin, “Rapid interpretation of EKG's: an interactive course,” Cover Publishing Company, 2000.

[6] H. Ashouri, and O. T. Inan, "Automatic detection of seismocardiogram sensor misplacement for robust pre-ejection period estimation in unsupervised settings”, IEEE sensors journal, vol. 17, no. 12, pp. 3805-3813, 2017.

[7] R. P. Patterson, "Fundamentals of impedance cardiography", IEEE Engineering in Medicine and Biology magazine, vol. 8, no. 1, pp. 35-38, 1989.

[8] I. Starr, A. J. Rawson, H. A. Schroeder, and N. R. Joseph, “Studies on the estimation of cardiac output in man, and of abnormalities in cardiac function, from the heart’s recoil and the blood’s impacts; the ballistocardiogram,” American Journal of Physiology-Legacy Conten, vol. 127, pp. 1–28, 1939.

[9] J. W. Gordon, “Certain molar movements of the human body produced by the circulation of the blood,” Journal of anatomy and physiology, vol. 11, no. Pt3, pp. 533–536, 1877.

[10] J. Q. Wang, C. X. Zheng, X. J. Jin, G. H. Lu, and A. S. Ni, “Study on a non-contact life parameter detection system using millimeter wave,” Journal of Space Medicine & Medical Engineering of China, vol. 17, pp. 157–161, 2004.

[11] O. T. Inan, M. Etemadi, R. M. Wiard, L. Giovangrandi, and G. T. A. Kovacs, "Robust ballistocardiogram acquisition for home monitoring," Physiological measurement, vol. 30, no. 2, pp. 169, 2009.

[12] D. Shao, F. Tsow, C. Liu, Y. Yang, and N. Tao, "Simultaneous monitoring of ballistocardiogram and photoplethysmogram using a camera," IEEE Transactions on Biomedical Engineering, vol. 64, no. 5, pp. 1003-1010, 2016.

[13] E. S. Winokur, D. D. He, and C. G. Sodini, “A wearable vital signs monitor at the ear for continuous heart rate and pulse transit time measurements,” Annual International Conference of the IEEE Engineering in Medicine and Biology Society, pp. 2724–2727, 2012.

[14] Ł. Dziuda, M. Krej, and F. W. Skibniewski, "Fiber Bragg grating strain sensor incorporated to monitor patient vital signs during MRI," IEEE Sensors Journal, vol. 13, no. 12, pp. 4986-4991, 2013.

[15] Effects of slow breathing rate on heart rate variability and arterial baroreflex sensitivity in essential hypertension.

[16] W. Lyu, F. Tan, S. Chen, and C. Yu, “Myocardial contractility assessment using fiber optic sensors,” Asia Communications and Photonics Conference and Exhibition (ACP), Paper M4A.152, pp. 1-3, 2019.

[17] J. Gomez-Clapers, A. Serra-Rocamora, R. Casanella, and R. Pallas-Areny, “Towards the standardization of ballistocardiography systems for J-peak timing measurement,” Measurement, vol. 58, pp. 310-316, 2014.

[18] M. Etemadi, O. T. Inan, L. Giovangrandi, and G. T. A. Kovacs, “Rapid assessment of cardiac contractility on a home bathroom scale,” IEEE Transactions on Information Technology in Biomedicine, vol. 15, no. 6, pp. 864–869, 2011.